Anal. Chem. **2009,** *81,* 7141–7148

Accelerated Articles

Protein Quantification in Complex Mixtures by Solid Phase Single-Molecule Counting

Lee A. Tessler,[†] Jeffrey G. Reifenberger,[‡] and Robi D. Mitra*,[†]

Center for Genome Sciences, Department of Genetics, Washington University in St. Louis School of Medicine, 4444 Forest Park Avenue, St. Louis, Missouri 63108, and Helicos Biosciences, One Kendall Square, Cambridge, Massachusetts 02139

Here we present a procedure for quantifying single protein molecules affixed to a surface by counting bound antibodies. We systematically investigate many of the parameters that have prevented the robust single-molecule detection of surface-immobilized proteins. We find that a chemically adsorbed bovine serum albumin surface facilitates the efficient detection of single target molecules with fluorescent antibodies, and we show that these antibodies bind for lengths of time sufficient for imaging billions of individual protein molecules. This surface displays a low level of nonspecific protein adsorption so that bound antibodies can be directly counted without employing two-color coincidence detection. We accurately quantify protein abundance by counting bound antibody molecules and perform this robustly in real-world serum samples. The number of antibody molecules we quantify relates linearly to the number of immobilized protein molecules ($R^2 = 0.98$), and our precision (1−5% CV) facilitates the reliable detection of small changes in abundance (7%). Thus, our procedure allows for single, surface-immobilized protein molecules to be detected with high sensitivity and accurately quantified by counting bound antibody molecules. Promisingly, we can probe flow cells multiple times with antibodies, suggesting that in the future it should be possible to perform multiplexed single-molecule immunoassays.

Our ability to detect and quantify proteins has lagged behind our ability to analyze nucleic acids. Closing this gap by developing more sensitive and quantitative protein analysis methods would greatly aid efforts to understand cellular processes[1,2] and to search for protein biomarkers that reveal disease state.[3,4] The application of single-molecule detection (SMD) methods to proteins holds great promise in this regard for five reasons: (1) Recent advances have made SMD methods inexpensive, robust, and reliable.[5,6] (2) SMD methods can enable the detection of low-abundance proteins,[7−9] which is especially important because the poor sensitivities of current proteomic methods are limiting progress in the area of biomarker discovery.[10,11] (3) SMD methods can enable protein quantification by employing single-molecule counting, which can be significantly more accurate than bulk methods.[12,13] (4) SMD methods can enable analysis of protein−protein interactions by detecting single-molecule colocalization.[14] (5) SMD methods for proteins affixed to a surface could enable highly multiplexed immunoassays. For example, by creating ∼20 overlapping pools of labeled antibodies using a logarithmic pooling strategy like the one used to decode bead-based random microarrays,[15] a single assay could detect the protein targets of all 6 000 nonredundant human proteome antibodies[16] with only ∼20 binding rounds.

There are several obstacles that have hampered the development of single-molecule immunoassays. One is the lack of a good surface for the SMD of surface-immobilized proteins. An ideal surface would be resistant to nonspecific antibody adsorption,

* Corresponding author. E-mail: rmitra@genetics.wustl.edu. Phone: (314)-362-2751. Fax: (314) 362-2156.

† Washington University in St. Louis School of Medicine.

‡ Helicos Biosciences.

(1) Ghaemmaghami, S.; Huh, W.; Bower, K.; Howson, R. W.; Belle, A.; Dephoure, N.; O'Shea, E. K.; Weissman, J. S. *Nature* **2003**, *425*, 737–741.

(2) Cohen, A. A.; Geva-Zatorsky, N.; Eden, E.; Frenkel-Morgenstern, M.; Issaeva, I.; Sigal, A.; Milo, R.; Cohen-Saidon, C.; Liron, Y.; Kam, Z.; Cohen, L.; Danon, T.; Perzov, N.; Alon, U. *Science* **2008**, *322*, 1511–1516.

(3) Omenn, G. S.; States, D. J.; Adamski, M.; Blackwell, T. W.; Menon, R.; Hermjakob, H.; Apweiler, R.; Haab, B. B.; Simpson, R. J.; Eddes, J. S.; Kapp, E. A.; Moritz, R. L.; Chan, D. W.; Rai, A. J.; Admon, A.; Aebersold, R.; Eng, J.; Hancock, W. S.; Hefta, S. A.; Meyer, H.; Paik, Y. K.; Yoo, J. S.; Ping, P. P.; Pounds, J.; Adkins, J.; Qian, X. H.; Wang, R.; Wasinger, V.; Wu, C. Y.; Zhao, X. H.; Zeng, R.; Archakov, A.; Tsugita, A.; Beer, I.; Pandey, A.; Pisano, M.; Andrews, P.; Tammen, H.; Speicher, D. W.; Hanash, S. M. *Proteomics* **2005**, *5*, 3226–3245.

(4) Anderson, L. *J. Physiol. (London, U.K.)* **2005**, *563*, 23–60.

(5) Harris, T. D.; Buzby, P. R.; Babcock, H.; Beer, E.; Bowers, J.; Braslavsky, I.; Causey, M.; Colonell, J.; Dimeo, J.; Efcavitch, J. W.; Giladi, E.; Gill, J.; Healy, J.; Jarosz, M.; Lapen, D.; Moulton, K.; Quake, S. R.; Steinmann, K.; Thayer, E.; Tyurina, A.; Ward, R.; Weiss, H.; Xie, Z. *Science* **2008**, *320*, 106–109.

(6) Roy, R.; Hohng, S.; Ha, T. *Nat. Methods* **2008**, *5*, 507–516.

(7) Sauer, M.; Zander, C.; Muller, R.; Ullrich, B.; Drexhage, K. H.; Kaul, S.; Wolfrum, J. *Appl. Phys. B: Lasers Opt.* **1997**, *65*, 427–431.

(8) Li, L.; Tian, X.; Zou, G.; Shi, Z.; Zhang, X.; Jin, W. *Anal. Chem.* **2008**, *80*, 3999–4006.

(9) Loscher, F.; Bohme, S.; Martin, J.; Seeger, S. *Anal. Chem.* **1998**, *70*, 3202–3205.

(10) Moul, J. W. *Clin. Prostate Cancer* **2003**, *2*, 87–97.

(11) Munkarah, A.; Chatterjee, M.; Tainsky, M. A. *Curr. Opin. Obstet. Gynecol.* **2007**, *19*, 22–26.

(12) Wold, B.; Myers, R. M. *Nat. Methods* **2008**, *5*, 19–21.

(13) Marioni, J. C.; Mason, C. E.; Mane, S. M.; Stephens, M.; Gilad, Y. *Genome Res.* **2008**, *18*, 1509–1517.

(14) Wallrabe, H.; Periasamy, A. *Curr. Opin. Biotechnol.* **2005**, *16*, 19–27.

10.1021/ac901068x CCC: $40.75
Published on Web 07/14/2009

while still allowing for the specific binding of antibodies to their target molecules. Efforts have been made to develop better surfaces,[17−28] however, the nonspecific adsorption on these surfaces has not been characterized with single-molecule resolution, with a few exceptions.[18,19] To work around high background surfaces, researchers have introduced innovative detection schemes, often relying on two-color coincidence detection.[29,30] This helps to reduce detection noise but is suboptimal for a proteomic method, since (1) pairs of protein-specific capture reagents with nonoverlapping epitopes may not be obtainable for all proteins, (2) generating pairs of reagents increases cost, and (3) determining the optimal binding conditions for dual antibody sandwich immunoassays can require more optimization than for single-capture antibody immunoassays.[31] A second obstacle to single-molecule immunoassays is the dissociation of antibodies from their individual targets during imaging. Many antibodies rapidly dissociate from their ligands in solution, but surface dissociation is often slower. It is not known whether the surface dissociation rates of antibodies will enable the sensitive detection of single ligand molecules. Finally, a single-molecule immunoassay must be able to sample large number of molecules in each experiment to ensure accurate protein quantification and to maximize the dynamic range.

Here we demonstrate a method for quantifying protein molecules on a surface by counting bound antibodies. To achieve this, we first optimized an image acquisition and processing method for SMD of fluorescently labeled antibodies on the surface of a flow cell. Then we systematically evaluated 12 surface chemistries for single-protein detection. For each surface, we quantified the nonspecific adsorption of single antibody molecules and characterized the efficiency of target protein immobilization. We found that a chemically adsorbed bovine serum albumin (BSA) surface had the lowest nonspecific binding and still allowed for efficient protein sample attachment. Using this surface incorporated into a flow cell, we measured the fraction of immobilized proteins that could be detected by direct antibody binding and found that a high fraction of targets (at least 70%) were bound specifically. We directly measured the surface dissociation of antibodies from their ligands and found it to be highly suited for large scale single-molecule quantification. We further showed that proteins were accessible to antibody binding over multiple binding rounds. Finally, we were able to quantify immobilized proteins by directly counting bound antibody molecules. A sufficiently low level of background binding was observed such that single target molecules could be detected without employing two-color coincidence detection. We found this method was both accurate and sensitive: the number of antibody molecules counted was linearly related to the number of proteins ($R^2 = 0.98$), and as few as 55 ligand molecules per 1 000 μm^2 image (1.4 pg cm^{-2}) could be detected over the background. Our detection method showed robustness in the background of a complex biological fluid, and we demonstrated the accurate quantification of an endogenous protein within blood serum samples. Thus, we have resolved many of the issues that have limited the feasibility of solid phase single-molecule protein analysis and have demonstrated reliable protein quantification in biological samples by single molecule counting on a solid surface.

MATERIALS AND METHODS

Imaging. All experiments were performed on a Nikon TE-2000 inverted microscope fitted with a total internal reflection fluorescence (TIRF) illuminator (Nikon, Melville, NY). Two lasers, 532 nm/75 mW and 640 nm/40 mW were used for fluorescence excitation (Compass 215M, Cube-40C, Coherent, Santa Clara, CA). Illumination of the sample was controlled through a computer animated shutter (Prior Scientific, Rockland, MA). The 532 nm laser beam was attenuated by a ND 2 neutral density filter (Nikon, Melville, NY). The two beams were coupled into one end of an optical fiber cable using a dichroic mirror (Z532BCM, Chroma, Brattleboro, VT), with the other end of the cable attached to the TIRF illuminator. Before reaching the objective, each laser beam passed through a band-pass filter: HQ545/30 for the green laser and D635/30 for the red laser (Chroma, Brattleboro, VT). Objective type total internal reflection was achieved through a 60× TIRF oil objective with index of refraction 1.49 (Nikon, Melville, NY). The chemistry of the assay was performed in a flow cell (see Fluidics) mounted onto the microscope stage. When the lasers are experiencing TIR, an evanescent wave decays exponentially at the glass−water interface into the flow cell to a distance of about 300 nm. TIRF allows for the excitation of only surface-bound fluorophore-labeled antibodies and therefore reduces the overall fluorescence background. The emitted photons from the labeled antibodies were collected by the objective and passed through a dichroic mirror (custom Cy3/Cy5, Semrock, Rochester, NY) and an emission filter for either the green channel (HQ610/75, Chroma, Brattleboro, VT) or the red channel (LP02-647RU-25, Semrock, Rochester, NY). Light was then detected by a charge coupled device (CoolSnap ED, Roper Scientific, Tucson, AZ) which imaged a 140 μm by 100 μm (1 400 pixels × 1 000 pixels) region of the surface.

Immediately prior to image acquisition, the flow cell was washed with 600 μL of PBS and loaded with 600 μL of oxygen

(15) Gunderson, K. L.; Kruglyak, S.; Graige, M. S.; Garcia, F.; Kermani, B. G.; Zhao, C. F.; Che, D. P.; Dickinson, T.; Wickham, E.; Bierle, J.; Doucet, D.; Milewski, M.; Yang, R.; Siegmund, C.; Haas, J.; Zhou, L. X.; Oliphant, A.; Fan, J. B.; Barnard, S.; Chee, M. S. *Genome Res.* **2004**, *14*, 870–877.
(16) Berglund, L.; Bjoerling, E.; Oksvold, P.; Fagerberg, L.; Asplund, A.; Szigyarto, C. A. K.; Persson, A.; Ottosson, J.; Wernerus, H.; Nilsson, P.; Lundberg, E.; Sivertsson, A.; Navani, S.; Wester, K.; Kampf, C.; Hober, S.; Ponten, F.; Uhlen, M. *Mol. Cell. Proteomics* **2008**, *7*, 2019–2027.
(17) Lange, K.; Rapp, M. *Anal. Biochem.* **2008**, *377*, 170–175.
(18) Jung, S.; Angerer, B.; Loscher, F.; Niehren, S.; Winkle, J.; Seeger, S. *ChemBioChem* **2006**, *7*, 900–903.
(19) Heyes, C. D.; Kobitski, A. Y.; Amirgoulova, E. V.; Nienhaus, G. U. *J. Phys. Chem. B* **2004**, *108*, 13387–13394.
(20) Sofia, S. J.; Premnath, V.; Merrill, E. W. *Macromolecules* **1998**, *31*, 5059–5070.
(21) Akkoyun, A.; Bilitewski, U. *Biosens. Bioelectron.* **2002**, *17*, 655–664.
(22) Piehler, J.; Brecht, A.; Geckeler, K. E.; Gauglitz, G. *Biosens. Bioelectron.* **1996**, *11*, 579–590.
(23) Piehler, J.; Brecht, A.; Valiokas, R.; Liedberg, B.; Gauglitz, G. *Biosens. Bioelectron.* **2000**, *15*, 473–481.
(24) Taylor, S.; Smith, S.; Windle, B.; Guiseppi-Elie, A. *Nucleic Acids Res.* **2003**, *31*.
(25) Masson, J. F.; Liddell, P. A.; Banerji, S.; Battaglia, T. M.; Gust, D.; Booksh, K. S. *Langmuir* **2005**, *21*, 7413–7420.
(26) Lange, K.; Rapp, M. *Anal. Biochem.* **2008**, *377*, 170–175.
(27) Yanker, D. M.; Maurer, J. A. *Mol. Biosyst.* **2008**, *4*, 502–504.
(28) Scott, E. A.; Nichols, M. D.; Cordova, L. H.; George, B. J.; Jun, Y. S.; Elbert, D. L. *Biomaterials* **2008**, *29*, 4481–4493.
(29) Agrawal, A.; Deo, R.; Wang, G. D.; Wang, M. D.; Nie, S. M. *Proc. Natl. Acad. Sci. U.S.A.* **2008**, *105*, 3298–3303.
(30) Li, H. T.; Zhou, D. J.; Browne, H.; Balasubramanian, S.; Klenerman, D. *Anal. Chem.* **2004**, *76*, 4446–4451.
(31) Kingsmore, S. F. *Nat. Rev. Drug Discovery* **2006**, *5*, 310–320.

scavenger and blink-reduction system[32] to prevent dyes from photobleaching and blinking. Then images were acquired in the red and green fluorescence channels at five different positions across the length of the flow cell, with 0.5 s exposure. Custom software written in Metamorph (Molecular Devices, Sunnyvale, CA) and Matlab (Mathworks, Natick, MA) was used to analyze the locations and intensities of the fluorescent molecules (see Supporting Methods in the Supporting Information).

Fluidics. The analysis substrate was a 40 mm diameter, no. 1.5 glass slide (Erie Scientific, Waltham, MA). The substrate was epoxide-derivatized by the vendor unless otherwise specified in Preparation of Surfaces. The slide was loaded into a flow cell (FSC2, Bioptechs, Butler, PA) fitted with perfusion ports to allow for reagents to be passed over the surface. Reagents were flowed through by a custom-made negative pressure vacuum pump.

Target Proteins. The target proteins were polyclonal goat IgG molecules labeled with an average of eight Cy3 dyes per molecule. The nonspecific target proteins used as a negative control in the target binding accessibility assay were polyclonal rabbit IgG molecules labeled with Cy3. Proteins were obtained from Abcam (Cambridge, MA).

Serum Samples. The serum sample used for the spike-in quantification experiment was obtained from rabbit. The serum samples used for the endogenous protein quantification experiment were from preimmunized, week 4, and week 5 rabbits in an antibody production protocol (for an unrelated study) during which rabbits were immunized with antigen and adjuvant. All serum samples were obtained from 21st Century Biochemicals (Marlboro, MA).

Antibodies. The antibodies used in all experiments with the exception of the endogenous protein quantification experiment were polyclonal antigoat, labeled with Cy5. The antibodies used to detect endogenous rabbit IgG were polyclonal antirabbit, labeled with Cy5. All antibodies were obtained from Abcam (Cambridge, MA).

Preparation of Surfaces. A total of 12 surfaces were generated by protocols taken directly from or adapted from surface blocking protocols in the literature.[18−28] Nine of the surface chemistries were generated by the chemical attachment of primary amine groups of a polymer or small molecule to epoxide-derivatized glass. The epoxide-coated glass was loaded into the flow cell and washed in 600 μL of phosphate buffered saline pH 7.3 (PBS). The glass was reacted with one of the following solutions in PBS for 1 h at room temperature: 1% bovine serum albumin (BSA) (Fisher Scientific, Pittsburgh, PA), 1% BSA/0.1% cold water fish skin gelatin (Aurion, The Netherlands), 1 M glucose, 10% linear polyacrylamide (LPA) MW 1500 Da, 10% LPA MW 10 kDa, 10% LPA MW 1 MDa, 100 mg/mL amino-PEG (Sigma-Aldrich, St. Louis, MO), 200 μg/mL rabbit IgG (Abcam, Cambridge, MA), and 100 mg/mL aminodextran MW 500 kDa (CarboMer, San Diego, CA). These surfaces were then capped with 1 M Tris pH 8.0 for 20 min. Two of the surfaces were generated by the noncovalent adsorption of a polymer to the glass. Here the epoxide-coated glass was first capped with ethanolamine-HCl pH 8.0 for 20 min and then treated with one of the following solutions in PBS for 1 h at room temperature: 100 mg/mL dextran MW 5 kDa and 1% PEG MW 8 kDa (Sigma-Aldrich, St. Louis, MO). The carboxymethyl (CM) dextran surface was generated as previously described.[21]

Measuring Nonspecific Adsorption. A flow cell containing the surface to be tested was loaded with 600 μL, 100 ng/mL Cy5 antibody. The surface was exposed to the antibody in the dark for 25 min at room temperature. Then, unbound antibodies were removed with a 600 μL PBS wash, and the flow cell was imaged as described above.

Immobilizing Protein Samples. A chemically adsorbed BSA surface was formed as described above, and the surface was activated with 0.2 M 1-ethyl-3-(3-dimethylaminopropyl)carbodiimide hydrochloride (EDC) and 0.05 M *N*-hydroxysuccinimide (NHS) (Pierce, Rockford, IL) in sodium phosphate buffer pH 5.8 (SPB) for 10 min. Free EDC and NHS was washed away with 600 μL of SPB.

The attachment of the protein sample of interest to the activated surface was as follows. For immobilization of purified target protein, 100 ng/mL (unless otherwise specified) of target protein in PBS was loaded into the flow cell. To generate a standard curve of detection, dilutions of target protein in PBS were loaded into the flow cell. To generate a standard curve of detection for target protein in the presence of serum, dilutions of target protein were spiked-in to whole rabbit serum, and the spiked-in serum was loaded into the flow cell. To detect endogenous IgG in serum, whole rabbit serum was diluted 1:10^5 in PBS and loaded into the flow cell.

Proteins samples that were loaded into the flow cell were allowed to react with the surface for 10 min at room temperature, in the dark. Then, unbound proteins were removed with a 600 μL PBS wash, and unreacted EDC-NHS sites on the BSA surface were quenched with 1 M Tris pH 8.0 for 20 min.

Antibody Binding and Oxygen Scavenging. After a protein sample was immobilized onto the flow cell surface (as described above), the Cy5-labeled antibody was loaded into the flow cell at 100 ng/mL (unless otherwise noted) in PBS and incubated for 2 h in the dark at room temperature. Unbound antibodies were washed away, and the flow cell was imaged.

RESULTS AND DISCUSSION

There are a number of formats and methods by which the SMD of biomolecules can be achieved.[33] We chose total internal reflection fluorescence microscopy as the basis for our single-molecule immunoassays. We attach a small amount of protein sample to the surface of a flow cell, probe with fluorescent antibodies, remove unbound antibodies, and directly image the bound antibodies (Figure 1A).

Iterative Thresholding Improves Detection of Labeled Antibody Molecules. We first sought to verify that our detection system could achieve single-molecule resolution of fluorescent antibody molecules affixed to glass. We mixed Cy3-labeled antibodies with identical antibodies labeled with Cy5, diluted the mixture, and reacted it to an epoxide-coated glass slide. We performed TIRF imaging with Cy3 and Cy5 channels, determined the positions of the Cy3 and Cy5 antibodies using software, and overlaid the positions (Figure S-1 in the Supporting Information). The Cy3-labeled molecules did not colocalize with Cy5-labeled

(32) Rasnik, I.; McKinney, S. A.; Ha, T. *Nat. Methods* **2006**, *3*, 891–893.

(33) Walter, N. G.; Huang, C. Y.; Manzo, A. J.; Sobhy, M. A. *Nat. Methods* **2008**, *5*, 475–489.

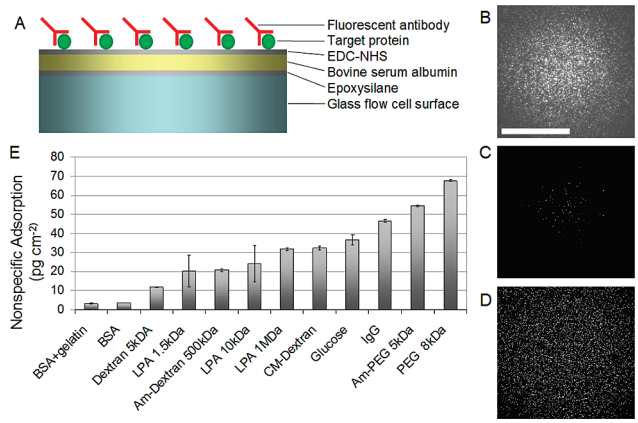

Figure 1. (A) Illustration of the single-molecule immunoassay. A chemically adsorbed BSA surface was prepared by reacting BSA with an epoxide-coated glass slide within a flow cell. Unreacted epoxides were quenched, and the BSA was activated for sample immobilization by EDC/NHS. The protein sample (circles) was immobilized to the BSA surface, and unreacted sites were passivated. The flow cell was probed with fluorescently labeled antibody and imaged. (B) The raw TIRF image of Cy5-labeled antibodies (scale bar = 50 μm) illustrates the nonuniform TIRF illumination. (C) Image processing by standard, single value thresholding allowed only a small portion of the raw image (the brightest spots) to be used for molecule identification. (D) Image processing by iterative thresholding allowed for most of the raw image (regardless of intensity) to be used for molecule identification. (E) Nonspecific adsorption of antibodies onto 12 surface protocols. Molecules were counted in $5 \times 1\,000$ μm^2 images, and units were converted to picograms per cm^2 assuming a 155 kDa molecular weight. The chemically adsorbed BSA surfaces suppressed nonspecific adsorption the most.

molecules more than would be expected by chance ($p = 0.78$, Fisher's Exact Test), demonstrating that the fluorescence objects detected were not clusters of antibodies (which would have been detected as colocalized molecules) but single antibody molecules.

In these initial experiments, we observed considerably fewer fluorescent antibodies at the edges of our field of view relative to the center of the image. This is due to the nonuniform laser illumination intrinsic to our Nikon optical design (Figure 1B). Since this nonuniform illumination greatly reduces the number of antibody molecules that can be analyzed in a single field of view using standard, single value thresholding, we developed an automated and unbiased image processing technique, "iterative thresholding" (see the Supporting Methods in the Supporting Information). The algorithm uses local thresholds to compensate for the lower intensities at the edges and is able to accurately identify the locations of fluorescent antibodies independent of their position within the field of view. We tested the performance of this technique by comparing images processed with our iterative thresholding algorithm with the same images analyzed by single value thresholding. Our iterative thresholding algorithm (Figure 1D) identified the positions of 14-fold more antibodies per field of view (1 408% ± 420%), on average, than the standard method (Figure 1C) while introducing few false positives with respect to the raw data (sensitivity = 99.96% ± 0.07%, specificity = 98.47% ± 0.76%). Thus iterative thresholding substantially increased the efficiency of fluorescent antibody analysis using objective TIRF and provided a foundation for our protein quantification method.

Study of Surface Nonspecific Adsorption. Minimizing the nonspecific adsorption of antibodies to surfaces is critical for the development of single-molecule immunoassays because it causes false positive events, decreasing the accuracy and sensitivity of the assays. To find the best surface for single-molecule immunoassays, we systematically searched the literature to identify surfaces that were shown to have minimal interactions with antibodies. We chose surface chemistries previously used for SMD[19] and for biosensors,[17,21,22,25] as well as several that we speculated would exhibit low levels of nonspecific protein adsorption. Some protocols were followed directly from the literature while others, such as the chemically adsorbed BSA protocols, were modified (see Materials and Methods).

We quantified the nonspecific adsorption of antibodies for 12 different surface chemistries. We loaded a glass slide into a flow cell, treated it according to a particular surface protocol, exposed it to Cy5-labeled antibody, washed away unbound antibodies, and quantified the number of adsorbed antibody molecules by single-molecule counting (Figure 1E). Since no ligand was present on the surface of the slide, each surface-bound antibody represented a nonspecific adsorption event. We observed 122−2 600 antibodies per 1 000 μm^2, (3−68 pg cm^{-2}). We found that a chemically adsorbed BSA surface (first developed by Heyes et al.[19] and modified here to allow adsorption to the glass via epoxide cross-linking and capping) showed the least amount of nonspecific binding. Dextran, aminodextran, and linear polyacrylamide (LPA) surfaces showed moderate adsorption. Among the LPA surfaces, polymers of lower molecular weight outperformed those of higher molecular weight. CM-dextran, glucose, IgG, amino-PEG, and PEG performed the worst.

These finding were consistent with those reported by Heyes et al.,[19] who found that chemical immobilization of BSA onto a glass surface provided great reduction in nonspecific adsorption of streptavidin molecules. By atomic force microscopy, they showed that this surface was highly homogeneous, supporting the hypothesis that the 75 kDa BSA protein creates a neutral, hydrophilic layer that sterically hinders proteins from nonspecifically adsorbing to the sticky silicon dioxide below. On the basis of the performance of our adapted BSA surface, we selected the chemically adsorbed BSA surface for further characterization.

Robust Immobilization of Protein Ligands on BSA-Coated Glass. It is important that a single-molecule immunoassay surface allows for the robust anchoring of ligand molecules. However, it was not clear whether the low background BSA surface discussed above could provide enough functional groups for the attachment of a protein sample. Therefore, we tested how efficiently proteins would anchor to the BSA surface using the heterobifunctional

cross-linking system 1-ethyl-3-(3-dimethylaminopropyl)carbodiimide hydrochloride (EDC) and *N*-hydroxysuccinimide (NHS). We prepared a BSA surface in a flow cell and activated the free carboxyl groups on the BSA molecules with EDC and NHS. We washed the flow cell to remove unbound cross-linker and then exposed the flow cell to Cy3-labeled protein to immobilize the proteins via their primary amines. The flow cell was washed again to remove unbound protein molecules, unreacted cross-linking sites were quenched, and the flow cell was imaged.

Cross-linking proteins to the BSA surface allowed for a 10-fold increase in the number of protein molecules affixed to the surface compared to the surface without EDC/NHS activation (950% ± 52%). Also, the proteins were able to be attached at over 1 000 molecules per field of view: a density that allows for high-throughput single-molecule sampling (Figure S-2 in the Supporting Information). Thus, we concluded that the EDC/NHS system was able to effectively activate the BSA surface and attach a protein sample. The chemically adsorbed BSA surface with EDC/NHS sample immobilization provided the surface chemistry for all subsequent experiments (Figure 1A).

We enable protein sample attachment by generating peptide bonds between the solvent-accessible carboxyl groups of the BSA and the primary amine groups of the target proteins. This contrasts the approach of some single-molecule studies which have relied on biotin streptavidin linkage.[19,34] Our method does not rely on prelabeling samples by biotinylation, instead taking advantage of endogenous lysine residues present on most proteins. Therefore our approach may provide a more universal way of attaching heterogeneous biological samples.

Efficient Detection of Single Protein Molecules by Antibody Binding. The accuracy of a single-molecule immunoassay depends on the accessibility of target molecules to antibodies; inaccessible ligands will not be detected or counted. There are several mechanisms that can prevent an antibody from binding a ligand immobilized on a solid substrate. Steric, electrodynamic, and thermodynamic variables can hinder binding when repulsive forces of the surface overcome the attractive forces of the antibody−protein complex. Kinetics can also hinder binding if a free energy barrier is sufficiently high to prevent docking on relevant time scales.[35] We sought to determine to what degree these variables affect the accessibility of target molecules to antibodies in our system.

To analyze the binding of target molecules by antibodies, we performed a dual-color, single-molecule protein accessibility assay (Figure 2). Here, the target proteins were labeled with Cy3 and the antibodies were labeled with Cy5. We prepared a BSA surface within a flow cell, immobilized the target proteins, capped the reactive cross-linking sites, and acquired a preantibody image. Then, we probed with antibodies, washed away unbound antibodies, and imaged. We compared the positions of the antibodies with the positions of the proteins imaged beforehand by overlaying their locations. To verify that the colocalization of proteins and antibodies was a result of specific binding, we measured the correlation between protein and antibody positions and tested that correlation for randomness (see Supporting Methods in the Supporting Information). The correlogram in Figure 2 indicates that antibody binding was specific and not due to chance correlation. (To confirm the specificity of binding we also performed the protein accessibility assay using a nonspecific target protein with which the antibodies should have had no affinity and observed a correlogram showing no significant correlations (Figure S-3 in the Supporting Information).)

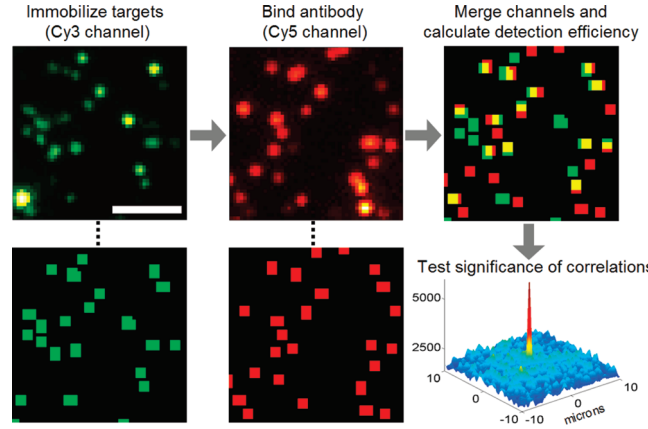

Figure 2. Determination of protein accessibility (detection efficiency). The image series illustrates target immobilization, antibody binding, and correlation detection. Each frame is an image of the same position in the flow cell (scale bar = 2 μm) and shows ~21 of the ~10^3 targets analyzed in each binding experiment. (i) After target protein immobilization, images of the Cy3-labeled proteins were acquired (top), and the positions of the proteins were determined by software (bottom). (ii) The surface was probed with antibody, images of bound Cy5-labeled antibodies were acquired (top), and positions of the antibodies were determined by software (bottom). (iii) Positions of the targets (green) and antibodies (red) were overlaid. Yellow pixels represent the colocalized molecules, indicating antibody-bound proteins. (iv) The correlogram analysis of this flow cell indicated that protein and antibody colocalization was nonrandom (i.e., antibodies were specifically binding to targets).

To quantify ligand accessibility, we measured the fraction of proteins that were colocalized with antibodies. We then performed this protein accessibility assay for different antibody concentrations. The total fraction of proteins bound by antibodies is shown by the dashed line in Figure 3. To better determine the amount of specific binding, we estimated nonspecific binding based on the observed antibody density and subtracted that from the total binding (see Supporting Methods in the Supporting Information). The dotted line shows the estimated fraction of proteins that overlapped with antibodies as a result of nonspecific binding, while the solid line shows the fraction of specifically bound ligand molecules.

The accessibility curve follows the behavior of fractional occupancy that is expected from binding theory. When 1 μg/mL antibody is used, ~70% of the target molecules were specifically bound by antibodies. From these results, we conclude that single protein molecules can be efficiently detected by counting bound antibody molecules.

Surface Dissociation of Antibodies. We sought next to determine if the ligand molecules that we failed to detect in the protein accessibility experiments described above were not detected because they were never bound by antibodies or if they were initially bound by antibodies but the complexes dissociated before imaging. Antibody−ligand interactions are known to have

(34) Braslavsky, I.; Hebert, B.; Kartalov, E.; Quake, S. R. *Proc. Natl. Acad. Sci. U.S.A.* **2003**, *100*, 3960–3964.
(35) Heyes, C. D.; Groll, J.; Moller, M.; Nienhaus, G. U. *Mol. Biosyst.* **2007**, *3*, 419–430.

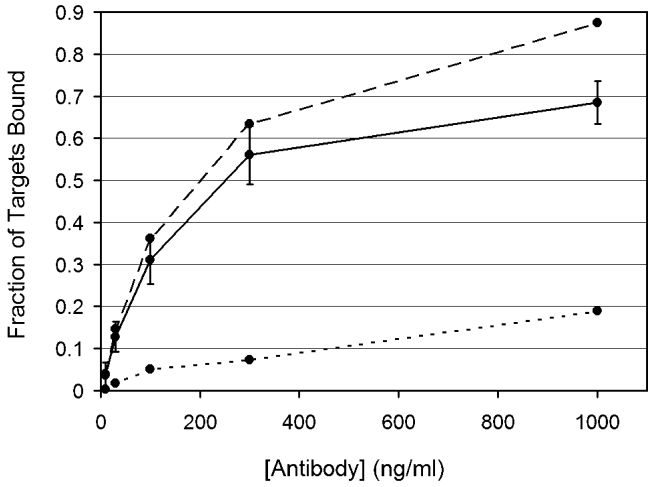

Figure 3. Protein accessibility (detection efficiency) as a function of antibody concentration. Specific binding (solid) was calculated by subtracting the nonspecific binding (dotted) from total binding (dashed). We could specifically bind as much as ~ 70% of the target molecules, enabling efficient protein detection.

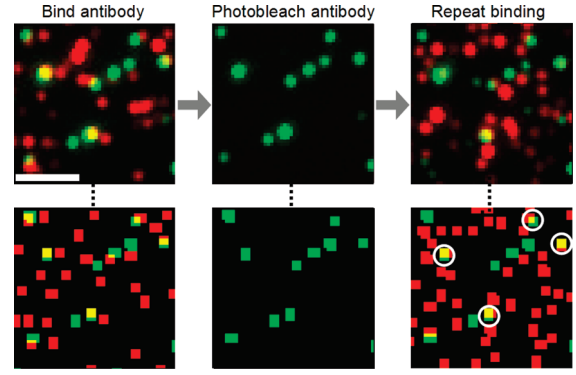

Figure 4. Protein rebinding. The image series illustrates two binding rounds separated by a photobleaching step (scale bar = 2 μm). Top: Raw images of Cy3 (green) and Cy5 (red) channels. Yellow represents merged channels. Bottom: Analyzed positions of protein molecules (green), antibody molecules (red), and colocalized antibody−protein molecules (yellow). Circles indicate proteins that were bound in both rounds. (i) First round of antibody binding detects immobilized proteins. (ii) Antibodies are photobleached. (iii) Second round of antibody binding detects many of the same proteins. We found that our surface allows for two successful rounds of binding.

dissociation half-lives in solution ranging from minutes to several hours. However, the surface dissociation rate may be slower due to surface−antibody interactions that stabilize the complex. Therefore, we designed an experiment to measure the surface dissociation rate of antibodies bound to single ligand molecules.

To measure the surface dissociation rate of the antibodies, we allowed antibodies to bind to target proteins that were immobilized on the surface of the flow cell, as previously described. We imaged the surface to determine the starting number of antibody−ligand complexes and then began a continual wash to remove unbound antibodies from the flow cell. We imaged the surface every 8 h over a 48 h period. At each time-point we quantified the number of antibody−ligand complexes that were lost relative to the starting time point, and from this we measured the surface dissociation of the antibodies.

Nearly all (>90%) of the colocalized pairs of proteins and antibodies remained intact for 48 h at room temperature (Figure S-4 in the Supporting Information). Furthermore, antibody dissociation did not follow exponential decay over this time period. Together, these results suggest a strong antibody−surface interaction. The high stability of bound antibodies also explains how we were able to detect single ligand molecules with high efficiency (i.e., Figure 3) even though we thoroughly washed the flow cell.

The half-life of a typical antibody−ligand complex can be as short as several minutes in solution. Such rapid dissociation would pose a serious barrier to the development of a solid phase, single-molecule immunoassay because antibodies would be washed off of the surface of the flow cell before they could be detected. Fortunately, surface interactions appear to stabilize antibody−ligand interactions.

Using the observed surface dissociation rate, we calculated the dynamic range that can theoretically be achieved. If ligand molecules are immobilized at a density of 1 000 target molecules per image and 10 images are acquired per second (a rate possible with the current generation of charge-coupled device cameras), then one can acquire images of $1\,000 \times 0.9 \times 10 \times 60 \times 60 \times 48 =$ 1.5 billion target molecules while retaining 90% of the antibodies on the surface. Thus, the observed surface dissociation rate will support a dynamic range of 9 orders of magnitude. This suggests that it should be possible to develop single-molecule immunoassays with a high dynamic range.

Dual-Round Protein Binding. Ligand rebinding in successive binding rounds could be used to increase detection specificity or to enable efficient sample multiplexing.[15] However, as our surface dissociation experiments illustrated, it was difficult to remove bound antibodies from the surface. This was true even after washing with various antibody eluting reagents (data not shown). Therefore, we wanted to explore rebinding ligands by "erasing" antibodies from the surface via photobleaching. We believed rebinding after photobleaching might be possible because the antibodies we used was polyclonal and could theoretically bind multiple epitopes on a single ligand.

One hurdle to performing multiple binding rounds with an intermediate photobleaching step is that the antibodies that bind in the first round could competitively inhibit the binding of antibodies in subsequent rounds. To test whether competitive binding would be a major phenomenon, we probed Cy3-labeled ligand molecules with Cy5-labeled antibodies as described above and acquired the positions of the bound antibodies. We then photobleached the antibodies with 640 nm light before performing a second round of binding with the same antibody. (Target molecules were not bleached.) If antibodies competitively inhibited the second round of binding, then we should not have observed any ligand molecules that were bound in both rounds.

We observed 2 829 Cy3-labeled ligand molecules. Of these, 1 497 proteins were bound in round 1, 1 146 were bound in round 2, and 526 (18.6%) were bound twice. Assuming independent binding in round 1 and round 2, we would expect 21% of the ligands to be bound twice. Thus, approximately 87% of the proteins bound in round 1 were available for binding in round 2 (Figure 4). This result supports the feasibility of performing multiple rounds of single-molecule protein detection.

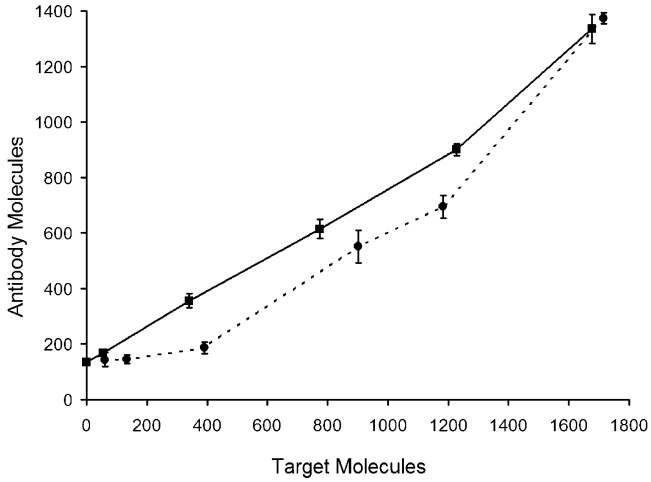

Figure 5. Single-molecule protein quantification. Solid line: We demonstrate a linear relationship between the number of antibody molecules and the number of protein molecules on the surface when detecting a purified protein sample. Linear fit $R^2 = 0.988$; coefficient of variation = 1−7%; lower limit of detection 55 molecules per 1 000 μm^2 image (1.4 pg cm^{-2}). Dashed line: We achieve accurate quantification in a complex protein sample. Detection of target protein spiked into undiluted rabbit serum produces a quantification curve that deviates only slightly from quantification of the purified sample. We did not observe any increase in background when detecting in serum.

Quantification of Single Molecules by Antibody Binding. We next set out to perform a quantitative immunoassay, counting single, immobilized protein molecules by detecting bound antibodies. We affixed varying amounts of Cy3-labeled protein onto the surface and quantified the number of immobilized target molecules by imaging. Then we probed the surface with Cy5-labeled antibodies and counted the total number of bound antibodies after washing.

The solid line in Figure 5 illustrates the relationship between number of antibody molecules and number of protein molecules affixed to the surface. In the range of 55 to 1 676 target molecules per 1 000 μm^2 image, we observed a linear relationship between the number target molecules and antibodies. The lower limit of detection (LOD) of 55 molecules per 1 000 μm^2 image (1.4 pg cm^{-2}) was achieved by acquiring only five images. It should be possible to detect lower quantities of surface-bound proteins by acquiring greater numbers of images.[8] Given our sample immobilization efficiency and this LOD, we were able to detect proteins in solution down to 100 pM. In this proof-of-principle study, we did not attempt to maximize the attachment efficiency but doing so should increase the detection sensitivity.[8]

The standard curve displays high correlation ($R^2 = 0.98$), and we obtain precision between 1% and 5% CV. By acquiring only five images, we can robustly detect abundance changes down to 7%; we generated 99% confidence intervals around each data point, and the widest interval was a 7% deviation. This result demonstrates the utility of digital quantification.

We also quantified the Cy3-labeled target protein in the presence of serum. Here, we spiked Cy3-labeled target protein at varying concentrations into neat rabbit serum. The complex mixture, including target and nontarget proteins, was immobilized to the BSA surface. We probed with fluorescently labeled antibody and quantified the number of target proteins versus the number of antibodies on the surface.

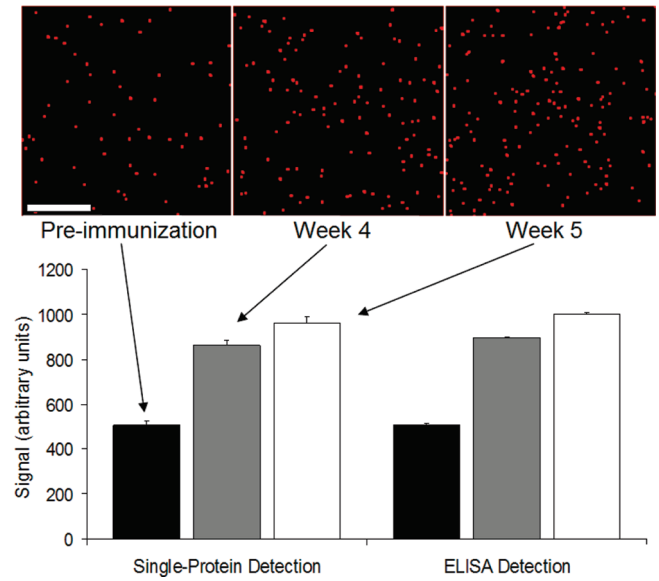

Figure 6. Quantification of endogenous IgG in serum. Using single-molecule protein quantification, we accurately measured the total IgG levels of a rabbit at various time points after immunization. Top: Single molecule counting at three time points (scale bar = 5 μm). We detected a 70.0% increase (±8.1%) in IgG levels between preimmunization and week 4, and a 11.7% increase (±4.4%) between weeks 4 and 5. Bottom: Bar graph representations of the above single-molecule counting data and of ELISA validation data (black = preimmunization; gray = week 4; white = week 5). Deviation of single-protein counting measurements from ELISAs were at most 4.2%. The single-molecule counting data and ELISA data were normalized to the preimmunization time point.

Similar results to the purified protein detection curve were obtained, demonstrating the robustness of the method in the presence of a complex biological fluid (Figure 5, dashed line). The LOD in serum was 390 molecules per 1 000 μm^2 (10 pg cm^{-2}) corresponding to a target starting concentration of 1 μg/mL. By comparison, the total concentration of the serum was 74 mg/mL (by dry weight). Therefore, despite the overabundance of serum proteins, the serum introduced almost no background. This indicates that single-antibody, direct binding can be used to make specific detection measurements in a highly complex biological fluid.

Accurate Quantification of an Endogenous Serum Protein. We next applied our method to quantify endogenous protein in a biological sample. We quantified the amount of total IgG in blood of a rabbit at various time points after immunization. Serum samples were diluted in PBS, immobilized to flow cell surfaces, and probed with antirabbit IgG Cy5-antibody. Then we quantified the antibodies remaining on the flow cell surface after washing.

We detected a 70.0% increase (±8.1%) in total IgG between preimmunization and week 4, as well as a subtle 11.7% increase (±4.4%) between weeks 4 and 5 (Figure 6). Our single-molecule quantitation measurements matched bulk measurements obtained by ELISA, deviating from the gold-standard by at most 4.2% (see Supporting Methods in the Supporting Information). This demonstrates the accuracy of single-molecule quantitation in complex, real-world samples.

CONCLUSION

Recent advances in SMD have the potential to usher in a new generation of proteomics tools. Toward the goal of uniting the field of protein detection with single-molecule counting, we present a proof-of-principle in which we quantify the abundance of individual proteins on a solid surface by counting bound antibodies. Further, we demonstrate quantitation of an endogenous protein in real-world serum samples while eliminating the need for two-color coincidence detection. We optimized key parameters, image acquisition and processing, nonspecific antibody adsorption, sample immobilization, sample accessibility, and surface dissociation, in a systematic way to enable a quantitative immunoassay. Because these parameters are interconnected, we found that it was important to optimize them simultaneously, which allowed us to quantify small changes (7%) in abundance of target proteins by single-molecule counting.

An important future goal is to perform multiple rounds of antibody binding on a solid surface to allow for efficient multiplexing.[15] This would be achieved by encoding each binding pool with a predetermined mixture of antibodies, so that n protein targets could be quantified in $\sim\log_2 n$ binding rounds (Figure S-5 in the Supporting Information). The ability to perform multiple rounds of binding would also enable error-checking, since antibodies would get a second pass at detecting a particular target. Additionally, analysis of protein−protein interactions would follow easily from such an approach, since interacting proteins will be present at the same positions on the flow cell.

Toward this goal, we have demonstrated the serial detection of proteins by two rounds of antibody binding. We used a photobleaching step after the first round of binding to erase surface-associated fluorescence prior to the second hybridization. We used photobleaching because the rate at which specifically bound antibodies dissociated from the surface was low enough that we found it difficult to completely remove them from the flow cell in a reasonable amount of time. Using this approach, we found that the majority (87%) of proteins that we expected to be bound in two binding rounds were in fact bound twice, indicating that competitive binding by the bleached, surface-bound antibodies was minimal. This lends support to the feasibility of multiple rounds of antibody binding and detection, with each round separated by a photobleaching step. (Alternatively, one could use a cleavable linker between the antibody and fluorophore, which would enable dye removal by exposure to a reducing agent or to light.[36])

Washing with surfactants and denaturants may allow us to better remove bound antibodies from their targets. For example, recent work demonstrated the efficient stripping of antibodies from Western blots without disrupting protein attachment.[37] To develop such a protocol in a single-molecule setting will require a low-background surface that is also surfactant-compatible (the surfaces described here are not). We are now investigating low-background surfactant-compatible surfaces that utilize multiarm PEG nanogels.[38]

Some obstacles still must be overcome before it is feasible to develop a multiplexed single-molecule immunoassay. For example, since each antibody−ligand pair has variable affinities, they each may need to be characterized beforehand in order to ensure that the concentration of antibody used in the immunoassay is high enough to ensure maximal binding to its immobilized ligand. However, as antibody production and characterization becomes more standardized, it will become possible to obtain large numbers of well-characterized antibodies. For example, the Human Antibody Initiative has already generated and curated antibodies against over 6 000 human proteins, and they aim to expand the collection to the entire human proteome within the decade.[16] Solid phase single-molecule immunoassays could provide a way to leverage such antibody collections toward high-throughput proteomic applications.

ACKNOWLEDGMENT

We thank Stan Lapidus and Patrice Milos for advice and helpful discussions. We thank Todd Druley, Jay Gertz, Katherine Varley, Haoyi Wang, and other members of the Mitra lab for helpful discussions and critical readings of the manuscript. This work was supported by Helicos Biosciences.

SUPPORTING INFORMATION AVAILABLE

Additional information as noted in text. This material is available free of charge via the Internet at http://pubs.acs.org.

Received for review May 15, 2009. Accepted July 1, 2009.

AC901068X

(36) Mitra, R. D.; Shendure, J.; Olejnik, J.; Edyta-Krzymanska-Olejnik; Church, G. M. *Anal. Biochem.* **2003**, *320*, 55–65.

(37) Yeung, Y. G.; Stanley, E. R. *Anal. Biochem.* **2009**, *389*, 89–91.

(38) Tessler, L. A.; Donahoe, C.; Elbert, D. L.; Mitra, R. D. 2009, in preparation.